Guided self-assembly of molecular dipoles on a substrate surface

Y. F. Gao and Z. Suo[a)]
Department of Mechanical and Aerospace Engineering and Princeton Materials Institute, Princeton University, Princeton, New Jersey 08544

(Received 3 October 2002; accepted 6 January 2003)

Molecules adsorbed on a substrate surface can self-assemble into a monolayer. This article models the process of self-assembly guided by an external object. The molecules are electric dipoles, diffusing on the surface at an elevated temperature. Pre-pattern a flat mask with a submonolayer of immobile atoms, which gives rise to a patterned contact potential field. Bring the mask to a small distance above the substrate. The electrostatic interaction transfers the pattern on the mask to a molecular pattern on the substrate. Similarly, one can place above the molecules a charged conducting tip, or a mask that is pre-patterned with a topographic surface. Our model includes the mobile molecular dipoles on the substrate surface, the guiding object, and the electrostatic field in the intervening space. A nonlinear diffusion equation simulates the pattern transfer process. Numerical results are presented when the guiding object is a flat metal, patterned with a submonolayer of immobile atoms. © *2003 American Institute of Physics.*
[DOI: 10.1063/1.1556190]

I. INTRODUCTION

Molecules adsorbed on a substrate surface are electric dipoles. At an elevated temperature, the molecules diffuse on the substrate surface, interact with one another through the intermolecular force, and self-assemble into a monolayer. The premise of this article is that an electric field, generated by an external object, can guide a submonolayer of the molecular dipoles to form patterns. The process is an example of *guided self-assembly*. This article investigates the process in a nonequilibrium thermodynamic framework.

Figure 1 shows one possibility of the theme. Above the molecules is placed a flat mask, which is pre-patterned with a submonolayer of atoms. A contact potential exists between a point in space neighboring a bare region on the mask and that neighboring a covered region.[1,2] For example, the adsorption of K on Pt (111) surface results in about 5 V contact potential relative to the bare Pt (111) surface.[3] Suppose that at an elevated temperature the atoms on the mask diffuse much slower than the molecular dipoles on the substrate. The submonolayer of adsorbed atoms on the mask gives rise to a fixed, patterned contact potential field, leading to a nonuniform electric field in the intervening space between the mask and the substrate. The electrostatic interaction between this electric field and the molecular dipoles will motivate the dipoles to diffuse on the substrate surface. The process transfers the pattern on the mask to a molecular pattern on the substrate. Figure 2 shows the plan view of some pre-patterns to be used in later simulations.

Section II develops a thermodynamic model that couples the mobile molecular dipoles on the substrate surface, the guiding object, and the electrostatic field in the intervening space. The electric field results from the external object and the nonuniform distribution of the molecular dipoles. If the guiding object is a flat metal, pre-patterned with a submonolayer of immobile atoms, the electrostatic field can be solved analytically in the Fourier space (Sec. III). Numerical simulations in Sec. IV follow the pattern transfer processes. When the space above the substrate is empty, a submonolayer of molecules on the substrate surface may separate into two phases, which self-assemble into various patterns.[4–14] With a mask, the phase patterns can be suppressed, and the mask patterns transferred (Sec. V). Section VI discusses the pattern transfer process in the context of existing experiments.

II. MODEL OF GUIDED SELF-ASSEMBLY

We extend a thermodynamic model[14] to couple the mobile molecular dipoles on the substrate surface, the guiding object, and the electrostatic field in the intervening space. The substrate occupies the space $x_3<0$, and its surface coincides with the plane (x_1,x_2). We assume that the submonolayer of molecular dipoles has negligible thickness. Describe the distribution of the molecules by a concentration field, $C(x_1,x_2)$, which varies continuously between 0 and 1. The guiding object, placed above the molecules, could be the mask with a contact potential pattern (Fig. 1). The intervening space between the molecules and the guiding object is filled with air, or with a dielectric liquid of permittivity ε. In what follows, we refer to the intervening space as the dielectric. Molecules move on the substrate surface by diffusion. The average concentration, C_0, remains constant during the process.

Write the free energy G of the system as

$$G=\int WdV-\int \Psi\rho dV+\int \Gamma dA-\int \phi^*\sigma^* dA^*. \quad (1)$$

The physical content of each term in Eq. (1) is prescribed as follows: W is the electrostatic energy per unit volume, and is

a)Author to whom correspondence should be addressed; electronic mail: suo@princeton.edu

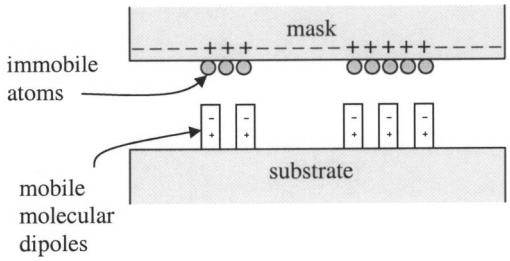

FIG. 1. Placing a mask above the substrate will guide the molecules to diffuse on the substrate surface. The mask is pre-patterned with a submonolayer of immobile atoms. The sizes of molecular dipoles and immobile atoms are exaggerated.

integrated over the volume of the dielectric. The electrostatic energy density is quadratic in the electric displacement D_i, namely,

$$W=\frac{1}{2\varepsilon}D_iD_i. \tag{2}$$

The Latin subscript runs from 1 to 3. The repeated subscript implies the summation convention. When the electric displacement varies by δD_i, the electrostatic energy density varies by

$$\delta W=E_i\delta D_i, \tag{3}$$

where E_i is the electric field. The electric field relates to the electric displacement as usual, i.e., $E_i=D_i/\varepsilon$.

In the dielectric the electric potential is $\Psi(x_1,x_2,x_3)$, and the electric charge per unit volume is ρ. The second integral in Eq. (1) also extends over the volume of the dielectric. It is the work done to move charge in the dielectric from zero potential to potential Ψ.

The third integral in Eq. (1) extends over the substrate surface. Assume that the interfacial free energy density Γ is a function of the concentration C, the concentration gradient ∇C, and the surface charge density σ. The charge distribution on the substrate surface can vary as electric current flows in the substrate. Expand the function Γ to the leading order power series in ∇C and σ

$$\Gamma=g+h|\nabla C|^2-\phi\sigma, \tag{4}$$

where g, h and ϕ are generally functions of C.

The function $g(C)$ is the free energy density of the interfacial system when the concentration field is uniform and the surface charge vanishes. This function accounts for the intermolecular interactions under such conditions. Regard the submonolayer as a binary solution. One component is the molecular dipoles, and the other is the bare substrate surface sites. Model the submonolayer as a regular solution, so that

$$g(C)=\Lambda k_BT[C\ln C+(1-C)\ln(1-C)]+\Lambda\omega C(1-C), \tag{5}$$

where Λ is the number of surface sites per unit area, k_B is Boltzmann's constant, and T is the absolute temperature. The parameter ω measures the magnitude of the enthalpy of mixing. When $\omega/k_BT<2$, the entropy of mixing prevails, and $g(C)$ has a single well. When $\omega/k_BT>2$, the enthalpy of mixing prevails, and $g(C)$ has two wells. If the average concentration C_0 is between the two wells, the molecules separate into two phases.

The concentration nonuniformity brings excess free energy. Following Cahn and Hilliard,[15] we represent this excess free energy by the term quadratic in the concentration gradient in Eq. (4). The symmetry excludes the term linear in the concentration gradient. The coefficient h is assumed to be a positive constant.

The quantity ϕ in Eq. (4) is the contact potential between a molecule-covered substrate surface and a bare substrate surface. Existing experiments[3,16–18] suggest that the contact potential is approximately linear in the concentration, namely,

$$\phi=\zeta C. \tag{6}$$

The slope ζ depends on the material system. As molecules diffuse on the substrate surface, electric current flows in the substrate to establish the surface charge distribution $\sigma(x_1,x_2)$. The term, $\phi\sigma$, is the work done per unit area to add surface charge σ. For a given concentration field, since ϕ is constant, the work done by ϕ reduces the free energy, as indicated by the negative sign in Eq. (4).

The quantities with asterisks in Eq. (1) are associated with the surface of the guiding object. In Fig. 1, ϕ^* is the prescribed contact potential field on the mask. The fourth integral in Eq. (1) represents the work done to add charge σ^* to the surface of the guiding object.

Given an electrostatic field in the dielectric, $\Psi(x_1,x_2,x_3)$, and the concentration field in the molecular submonolayer, $C(x_1,x_2)$, the above procedure calculates the free energy of the system. We next study the process by which the system approaches equilibrium.

A direct calculation gives the variation of the free energy

$$\delta G=\int\left(E_i+\frac{\partial\Psi}{\partial x_i}\right)\delta D_i dV-\int(\phi-\Psi)\delta\sigma dA-\int(\phi^*-\Psi)\delta\sigma^* dA^*+\int\left(\frac{\partial g}{\partial C}-2h\nabla^2C-\zeta\sigma\right)\delta C dA. \tag{7}$$

In deriving Eq. (7), we have applied divergence theorem, and Gauss's law, $D_{i,i}=\rho$. We have also discarded the integrals along lines on the substrate surface upon using the periodical boundary conditions.

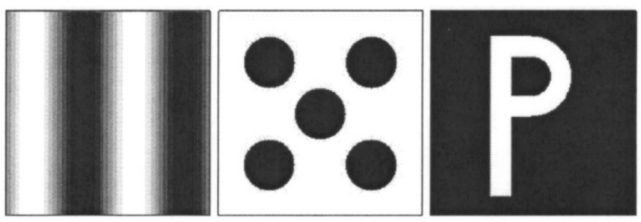

FIG. 2. Plan view of some pre-patterns on the mask in Fig. 1. Gray scale represents the prescribed contact potential field.

Molecular diffusion is a slow process compared with electric current flow in the substrate, so that the electric field is assumed to be in equilibrium. Consequently, the free energy variation associated with the variation in the electric displacement and the surface charge density vanishes. Equation (7) requires that

$$E_i = -\frac{\partial \Psi}{\partial x_i}, \quad \Psi|_A = \phi, \quad \Psi|_{A^*} = \phi^*. \tag{8}$$

These recover the familiar equations in electrostatics. We assume that the dielectric is free of charges, $\rho = 0$, so that the electric potential satisfies the Laplace equation, $\nabla^2 \Psi = 0$. Consequently, for a given concentration field, electrostatic equilibrium can be attained by solving the Laplace equation, subject to the boundary conditions ϕ and ϕ^*.

Applying Gauss's law to a small volume containing an element of the interfacial system at $x_3 = 0$, we obtain that the surface charge density relates to the electric potential in space as

$$\sigma(x_1, x_2) = -\varepsilon \frac{\partial \Psi}{\partial x_3}, \quad \text{at} \quad x_3 = 0. \tag{9}$$

The free energy variation associated with the variation in the concentration defines a thermodynamic force, driving the molecules to diffuse. Following Ref. 14, we derive a diffusion equation

$$\frac{\partial C}{\partial t} = \frac{M}{\Lambda^2} \nabla^2 \left(\frac{\partial g}{\partial C} - 2h \nabla^2 C - \zeta \sigma \right), \tag{10}$$

where M is the mobility of the molecules on the substrate surface. Diffusive equilibrium is attained by numerically integrating this nonlinear diffusion equation.

The comparison of the first two terms in the parenthesis of Eq. (10) defines a length scale: $b = (h/\Lambda k_B T)^{1/2}$. At room temperature, $k_B T \sim 5 \times 10^{-21}$ J. Following Suo, Gao, and Scoles,[14] we take $h \sim 10^{-21}$ J. $\Lambda^{-1/2}$ is of the molecular dimensions in the monolayer. Consequently, b is of the order of several angstroms. The time scale is $\tau = b^2/D_s = h/M(k_B T)^2$, where $D_s = M k_B T/\Lambda$ is the surface diffusivity.

A comparison of the last two terms in the parentheses of Eq. (10) determines another length scale

$$\lambda_0 = \frac{8\pi h}{\varepsilon \zeta^2}, \tag{11}$$

which measures the excess free energy due to the concentration nonuniformity relative to the electrostatic interaction. According to Evans *et al.*,[16,17] the contact potential variation is about 0.5 V for alkanethiols of different lengths or different terminal groups on Au (111) surface, so that we take $\zeta \sim 0.5$ V. The dielectric constant of vacuum is $\varepsilon = 8.854 \times 10^{-12}$ F/m. With these estimates, we obtain that λ_0 is on the order of 10 nm. If a high-permittivity liquid is filled in the intervening space, the length λ_0 reduces.

III. GUIDING WITH A FLAT, PRE-PATTERNED METAL

In Fig. 1, the mask occupies the space $x_3 > d$. The thickness of the atomic layer is also neglected, so that the mask surface is flat. The electrostatic boundary value problem can be solved analytically in the Fourier space. Represent the molecular concentration field on the substrate surface by a two-dimensional Fourier transformation

$$C(x_1, x_2, t) = \int_{-\infty}^{\infty} \int_{-\infty}^{\infty} \hat{C}(k_1, k_2, t) \times \exp(ik_1 x_1 + ik_2 x_2) dk_1 dk_2. \tag{12}$$

The real-valued concentration requires that $\hat{C}(k_1, k_2, t)$ and $\hat{C}(-k_1, -k_2, t)$ be complex conjugate. Pick up one such pair, and we obtain a concentration field, $C = 2\,\mathrm{Re}[\hat{C} \exp(ik_1 x_1 + ik_2 x_2)]$, where Re stands for the real part of a complex number. This concentration field represents an array of periodic stripes perpendicular to the vector (k_1, k_2).

Similarly write the Fourier transformation of the normalized contact potential field on the mask surface as

$$\phi^*/\zeta = U^*(x_1, x_2) = \int_{-\infty}^{\infty} \int_{-\infty}^{\infty} \hat{U}^*(k_1, k_2, t) \times \exp(ik_1 x_1 + ik_2 x_2) dk_1 dk_2. \tag{13}$$

Also pick up one pair of the Fourier components, namely, $U^* = 2\,\mathrm{Re}[\hat{U}^* \exp(ik_1 x_1 + ik_2 x_2)]$. We use ζ to normalize all electric potentials.

The electrostatic field in the dielectric depends on three spatial coordinates, but is a linear superposition of many Fourier components, each being a two-dimensional field. Consider the Fourier components of wavevectors (k_1, k_2) and $(-k_1, -k_2)$ only. The boundary condition at $x_3 = 0$ for the electrostatic field in the dielectric is

$$\Psi(x_1, x_2, 0) = 2\zeta\,\mathrm{Re}[\hat{C} \exp(ik_1 x_1 + ik_2 x_2)] \tag{14}$$

and that at $x_3 = d$ is

$$\Psi(x_1, x_2, d) = 2\zeta\,\mathrm{Re}[\hat{U}^* \exp(ik_1 x_1 + ik_2 x_2)]. \tag{15}$$

Matching those boundary conditions, the solution to the Laplace equation $\nabla^2 \Psi = 0$ gives the electric potential in the dielectric

$$\Psi(x_1, x_2, x_3) = 2\zeta\,\mathrm{Re}\{[A_1 \exp(-kx_3) + A_2 \exp(kx_3)] \times \exp(ik_1 x_1 + ik_2 x_2)\}, \tag{16}$$

where

$$A_1 = \frac{\hat{C} \exp(2kd) - \hat{U}^* \exp(kd)}{\exp(2kd) - 1}, \quad A_2 = \frac{\hat{U}^* \exp(kd) - \hat{C}}{\exp(2kd) - 1}. \tag{17}$$

Superimposing all the Fourier components, we obtain the solution for any arbitrary concentration field C and prescribed contact potential field ϕ^*.

Once the electric potential Ψ in the dielectric is determined, the charge density on the substrate surface is determined from Eq. (9), giving

$$\sigma = 2\varepsilon\zeta\,\mathrm{Re}\left\{ k \left[\frac{1}{\tanh(kd)} \hat{C} - \frac{1}{\sinh(kd)} \hat{U}^* \right] \times \exp(ik_1 x_1 + ik_2 x_2) \right\}. \tag{18}$$

Normalizing the time t by τ, the coordinates x_1 and x_2 by b, the free energy by $\Lambda k_B T$, and the surface charge density by $\varepsilon\zeta^2/b$, we rewrite the diffusion Eq. (10) in the Fourier space as

$$\frac{\partial \hat{C}}{\partial t} = -k^2\hat{P} - 2k^4\hat{C} + \frac{1}{\tanh(kd)} \times \eta k^3 \hat{C} - \frac{1}{\sinh(kd)}\eta k^3 \hat{U}^*, \tag{19}$$

where $\hat{P}(k_1,k_2)$ is the Fourier transformation of the function

$$P(C) = \log\left(\frac{C}{1-C}\right) + \frac{\omega}{k_B T}(1-2C) \tag{20}$$

and $\eta = 8\pi b/\lambda_0$ is a dimensionless parameter.

In Eq. (19), $\hat{U}^*$ is fixed, and affects diffusion like a static force. The Fourier component $\hat{U}^*(k_1,k_2)$ directly affects the corresponding Fourier component $\hat{C}(k_1,k_2)$. The other Fourier components of U^* indirectly affect $\hat{C}(k_1,k_2)$ through the nonlinear function $P(C)$. The Fourier component $\hat{U}^*(k_1,k_2)$ enlarges the magnitude of $\hat{C}(k_1,k_2)$ if they have opposite signs. The magnifying trend will be competed by the gradient energy, which is represented by the $-2k^4\hat{C}$ term. Consequently, the molecular dipoles will diffuse on the substrate, either toward the areas below the positively charged areas on the mask if the dipole moments are negative, or away from those areas if the dipole moments are positive, as indicated in our scheme (Fig. 1).

At a certain time, for a given concentration field, we first evaluate $\hat{C}$ and $\hat{P}$ by using the fast Fourier transformation (FFT), and then use Eq. (19) to update the concentration field for a small time step. Repeat the procedure for many time steps to evolve the concentration field over a long period of time. The inverse FFT is used to obtain the concentration field in the real space. The numerical results are presented in the following two sections.

IV. GUIDED SELF-ASSEMBLY OF A SUBMONOLAYER WITHOUT PHASE SEPARATION

When $\omega/k_B T < 2$ in Eq. (5), the molecules do not separate into distinct phases. We consider this behavior first and use $\omega/k_B T = 0$ in the simulation. Figure 3 shows the simulation results of the submonolayer guided by the mask pattern in Fig. 2(a), with a sinusoidal contact potential field

$$\phi^* = \phi_0 + 10\zeta \sin\left(\frac{2\pi x_1}{128b}\right), \tag{21}$$

where the period is $128b$, the average value is ϕ_0, and the amplitude is 10. The simulation is restricted within a $256b \times 256b$ square cell. The periodic boundary conditions replicate the square cell to the entire substrate surface. Let $\eta = 2$, $d = 2.5\lambda_0$, and $C_0 = 0.5$.

The initial concentration field on the substrate surface is uniform, so that $\Psi(x_1,x_2,0)/\zeta = C_0$. Constants C_0 and ϕ_0 lead to a uniform electric field in the dielectric, which does not affect the motion of the molecules. For convenience, let $\phi_0 = C_0 = 0.5$. Figure 3(a) plots the contours of the electric potential in the dielectric when the molecules are uniformly distributed on the substrate. The surface charge density is nonuniform, motivating the molecules to diffuse.

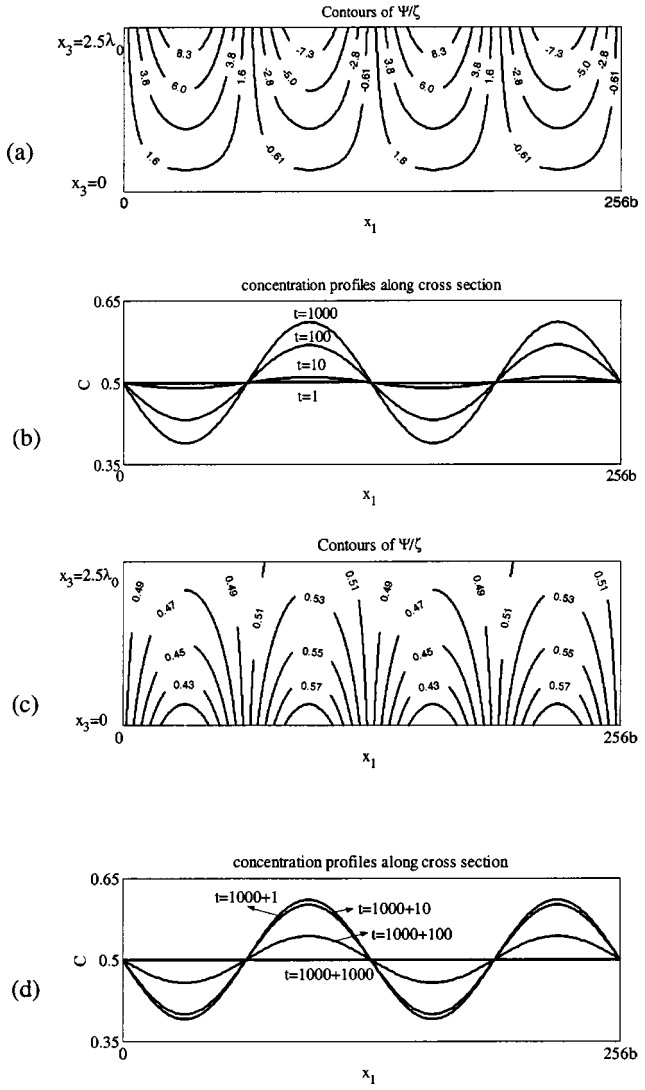

FIG. 3. (a) Contours of electric potential field in the dielectric, when the concentration field is uniform in the submonolayer; (b) guided by the mask pattern in Fig. 2(a), the concentration field modulates and reaches equilibrium at $t = 1000\tau$. Remove the mask at this time; (c) contours of electric potential field above the molecules; (d) relax the submonolayer.

As time goes on, the molecular distribution modulates, and reaches a wave-like equilibrium distribution around $t = 1000\tau$ [Fig. 3(b)]. The distributions at $t = 1000\tau$ and $t = 10\,000\tau$ are indistinguishable. The equilibrium concentration field is indeed out phase with the mask pattern, as expected.

Remove the mask at $t = 1000\tau$, and lower the temperature to freeze the molecular pattern. Figure 3(c) plots the electric potential contours in the space above the molecules. Along any horizontal plane in the space, the electric field is nonuniform. The molecular pattern can be recognized by sensing this electric field. Subsequently, when the temperature is elevated again, with no mask in the space, the submonolayer will relax to the uniform concentration field in about the same amount of time [Fig. 3(d)]. The two states—

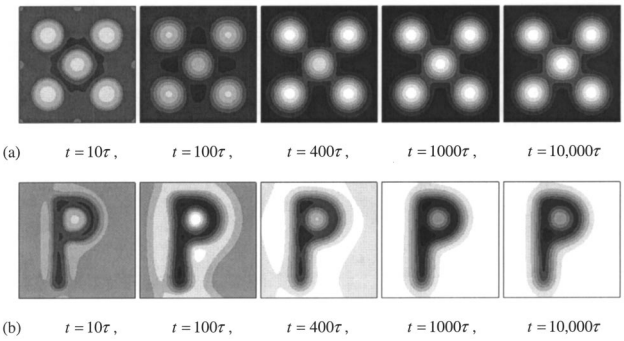

FIG. 4. Two evolution sequences of concentration fields ($C_0=0.5$). The mask patterns are Fig. 2(b) and 2(c), respectively.

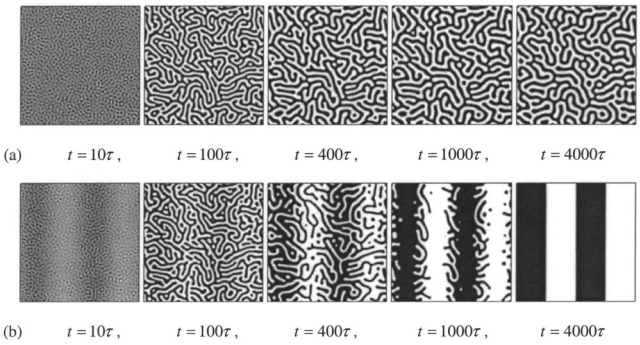

FIG. 5. Two evolution sequences of concentration fields ($C_0=0.5$): (a) without mask, (b) with mask pattern in Fig. 2(a).

the uniform and the nonuniform dipole distributions—can serve as a memory. The above steps constitute writing, reading, and erasing.

We have also tried two other mask patterns. Figure 2(b) prescribes five circles, each of radius $32b$. The pattern is roughly equivalent to packing five conducting tips together. Figure 2(c) prescribes a letter P as a mask pattern. The difference of U^* between bright and dark areas is 10. The other parameters used are the same as before. The simulation results are given in Figs. 4(a) and 4(b), respectively. A gray scale is adopted to visualize the concentration fields. The concentration fields also modulate and evolve to equilibrium molecular patterns. In Fig. 4(a), each circle on the mask induces a circular feature on the substrate, with a smoothly varying concentration field. Since the five circles are packed closely, the circular features on the substrate overlap somewhat. The letter P is asymmetric, having different Fourier components in every direction. Inspecting Eq. (19) again, we find that the coefficient for $\hat{U}^*(k_1,k_2)$ varies for different magnitude of wavevector (k_1,k_2), and all the Fourier components of the concentration field are coupled with each other through $P(C)$. This explains why the final molecular pattern in Fig. 4(b) is distorted from the mask pattern.

Obviously, the larger the gap between the substrate and the mask, the weaker the guidance. Not only does the pattern transfer process become slower, also the contrast of the equilibrium concentration field decreases. When the mask is moved far away, the concentration will no longer modulate. The larger the contact potential variation on the mask, the stronger the guidance. Moreover, when the mask pattern is coarse, the coefficient for $\hat{U}^*$ in Eq. (19) decreases, and then the pattern transfer process is slowed accordingly.

In the above simulation results, the concentration variations are about 0.2–0.4. Take $\zeta=0.5$ V, so that the variation of ϕ is about 0.1–0.2 V. The contrast of the contact potential field on the mask is $|\Delta U^*|=10$, corresponding to $|\Delta\phi^*|=5$ V. The gap, $d=2.5\lambda_0$, corresponds to several tens to hundreds of nanometers. Experiments have shown that the contact potential can vary from -1 to 5 V for different material systems.[3,16–18] For alkanethiols on gold surfaces, the observed islands ripening in an incomplete monolayer happens in the scale of hours,[11] indicating that surface diffusion is a slow process. However, surface diffusivity varies considerably with the material system and the temperature. Consequently, all the above parameters are in the realistic scope, so that the method for pattern transfer is plausible.

V. GUIDED SELF-ASSEMBLY OF A SUBMONOLAYER WITH PHASE SEPARATION

When $\omega/k_BT>2$ in Eq. (5), the molecules on the substrate can separate into two phases. In our earlier articles,[14,19] we have studied the dynamics of binary monolayers without any guiding object. The simulation assumes $\omega/k_BT=2.2$, so that $g(C)$ has two wells at $C_\alpha\approx0.25$ and $C_\beta\approx0.75$. Starting from a concentration field with small random perturbations from the average value C_0, the monolayer evolves into either meandering stripes, as shown in Fig. 5(a) when $C_0=0.5$, or polygrains of triangular lattices, as shown in Fig. 8(a) when $C_0=0.4$. The feature size is on the order of λ_0, and the phase boundary width is about $3b$. Further annealing improves the spatial ordering, but does not change the feature size. These intrinsic phase patterns are stabilized by the electrostatic field caused by the molecular dipoles, e.g., Fig. 3(c).

With a patterned mask placed above, the molecules form different patterns. First use the mask pattern in Fig. 2(a), with the contact potential field prescribed in Eq. (21). Let $d=3.5\lambda_0$, and $C_0=0.5$. Figure 5(b) shows the evolution sequences of molecules on the substrate. As times goes on, the fine phase patterns vanish. The equilibrium molecular pattern in Fig. 5(b) is clearly guided by the mask pattern. Figure 6 compares the equilibrium molecular distributions for the two cases, $\omega/k_BT=0$ and $\omega/k_BT=2.2$. Without phase separation, the equilibrium pattern is wave-like. With phase separation, the equilibrium pattern is step-like. Overshoots in Fig. 6 are probably due to the property of Fourier transformation. When the amplitude of the contact potential field on the mask increases, or the gap decreases, the amplitude of the wave-like curve in Fig. 6 also increases. However, the amplitude of the step-like one is roughly determined by the two phases. Figure 7 plots the contours of electric potential in the space, when the concentration field is step-like, and the mask is removed. Because of the phase separation, this field is quite different from that in Fig. 3(c).

We next use the mask pattern in Fig. 2(c). To accelerate the simulation process, we let the difference of U^* between

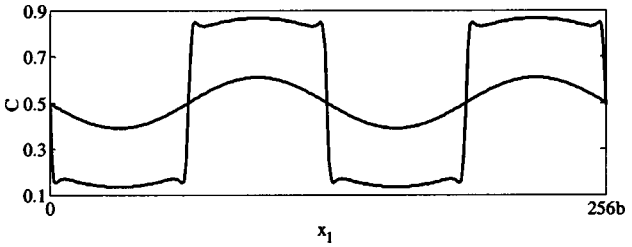

FIG. 6. Guided by the mask pattern in Fig. 2(a), the equilibrium concentration profile is wave-like without phase separation, or step-like with phase separation.

bright and dark areas be 1, and $d=\lambda_0/2$. The average concentration is $C_0=0.4$. Figure 8(b) shows the evolution sequences of the molecules on the substrate surface. Molecules can be significantly guided even before the two phases are fully separated. The small dots still remain outside the letter P. For some choices of parameters $|\Delta U^*|$ and d, the equilibrium molecular patterns are appreciably distorted. When the mask is far away molecules will not be guided. There should exist a transition from mask-induced pattern to intrinsic phase pattern. However, we have not carried out a comprehensive parametric study of this transition.

VI. DISCUSSION

Lithography makes structures with a resolution of several tens of nanometers. To fabricate structures at an even smaller scale, complicated and expensive improvements are needed. Alternatively, molecular self-assembly makes structures molecule by molecule. However, this method does not produce designed patterns at a length scale larger than the size of several hundreds of molecules. Guided self-assembly integrates the top-down and bottom-up strategies. Molecules on a substrate surface can be guided to form patterns by the electrostatic interaction between the molecular dipoles and an external object. The molecular patterns could serve as memories, or as templates for making devices.

We have presented the simulation results when the guiding object is the mask that is prepatterned with a submonolayer of atoms. The guiding object could also be a conducting tip, or a metal pre-patterned with a topographic surface. Figure 9(a) shows a charged conducting tip brought to a small distance above the molecules. The electrostatic interaction motivates the molecules to diffuse on the substrate surface, either toward the spot below the tip, or away from the spot. The idea is motivated by a recent IBM work.[20,21]

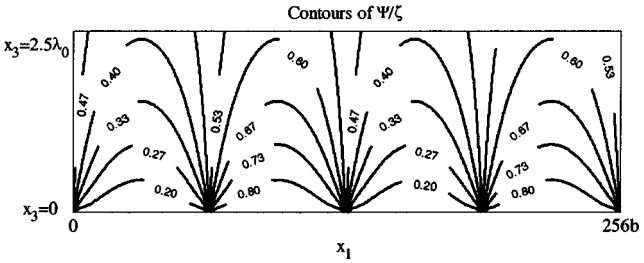

FIG. 7. Contours of electric potential field above the molecules when the concentration field is step-like.

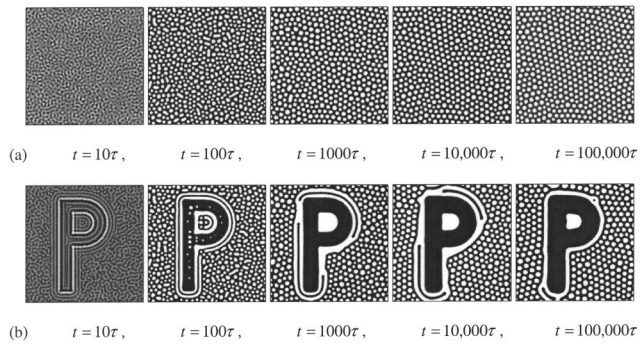

FIG. 8. Two evolution sequences of concentration fields ($C_0=0.4$): (a) without mask, (b) with mask pattern in Fig. 2(c).

They use a thin polymer film as the storage media. When heating up and applying a pressure with an atomic force microscopy cantilever, they can write by creating nanoscale indentations in the polymer. The same cantilever tip can be used to read by sensing the thermal resistance difference in the polymer layer due to the topographic profile. Our idea also differs from the work of Stroscio and Eigler.[22] They can manipulate individual atoms or molecules in a variety of ways by using the interactions present in the tunnel junction of a scanning tunneling microscope. In contrast to their typically 5 Å tip-substrate distance, our setup is of mesoscopic scale (several tens to hundreds of nanometers). The electrostatic interaction prevails, and motivates the motion of a large number of molecular dipoles.

Figure 9(b) illustrates another mechanism of pattern transfer. Above the molecules is placed a metallic mask, which is pre-patterned with a topographic surface. A voltage

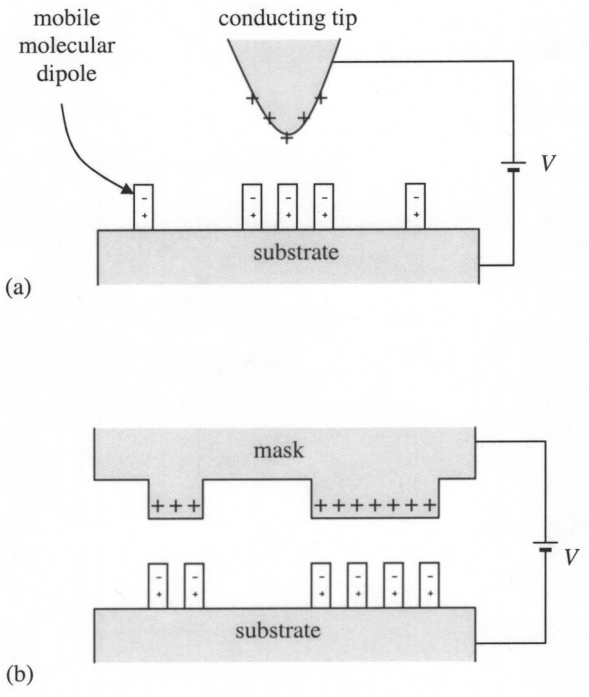

FIG. 9. Two other possibilities of guided self-assembly. Above the molecules is placed (a) a charged conducting tip; (b) a metallic mask, which is pre-patterned with a topographic surface.

is applied between the mask and the substrate. The protruding parts of the mask cause stronger electric fields between the mask and the substrate. Consequently, the molecules will be guided to diffuse on the substrate surface. The process transfers the topographic pattern on the mask to a molecular pattern on the substrate. This idea follows Chou and Zhuang[23] and Shäffer, Thurn-Albrecht, and Russell.[24] They placed a mask of topographic patterns above a smooth thin polymer film. After annealing, the initially flat polymer film self-assembled into periodic pillar arrays.

The process described in this article has some advantages. The storage media is a submonolayer, much thinner than the polymer film. Writing and erasing now involve diffusion on the surface, rather than flow in a film. Reading involves proximity sensing, rather than mechanical contact. Wear of the tip is not a concern. We eagerly await experiments to demonstrate that molecular dipoles assemble into a pattern, guided by a mask, or by a conducting tip.

ACKNOWLEDGMENTS

The work is supported by the Department of Energy through Grant No. DE-FG02-99ER45787, and by the National Science Foundation through the Material Research Science and Engineering Center.

[1] L. D. Landau, E. M. Lifshitz, and L. P., Pitaevskii, *Electrodynamics of Continuous Media*, 2nd ed. (Butterworth Heinemann, New York, 1984).
[2] N. W. Ashcroft and N. D. Mermin, *Solid State Physics* (Saunders College, Philadelphia, 1976).
[3] R. G. Windham, M. E. Bartram, and B. E. Koel, J. Phys. Chem. **92**, 2862 (1988).
[4] K. Kern, H. Niehus, A. Schatz, P. Zeppenfeld, J. Goerge, and G. Comsa, Phys. Rev. Lett. **67**, 855 (1991).
[5] R. Plass, J. A. Last, N. C. Bartelt, and G. L. Kellogg, Nature (London) **412**, 875 (2001).
[6] H. Ellmer, V. Repain, S. Rousset, B. Croset, M. Sotto, and P. Zeppenfeld, Surf. Sci. **476**, 95 (2001).
[7] J. P. Folkers, P. S. Laibinis, G. M. Whitesides, and J. Deutch, J. Phys. Chem. **98**, 563 (1994).
[8] S. J. Stranick, A. N. Parikh, Y. T. Tao, D. L. Allara, and P. S. Weiss, J. Phys. Chem. **98**, 7636 (1994).
[9] K. Tamada, M. Hara, H. Sasabe, and W. Knoll, Langmuir **13**, 1558 (1997).
[10] D. Hobara, M. Ota, S. Imabayashi, K. Niki, and T. Kakiuchi, J. Electroanal. Chem. **444**, 113 (1998).
[11] E. Barrena, C. Ocal, and M. Salmeron, J. Chem. Phys. **111**, 9797 (1999).
[12] D. Vanderbilt, Surf. Sci. **268**, L300 (1992).
[13] M. Seul and D. Andelman, Science **267**, 476 (1995).
[14] Z. Suo, Y. F. Gao, and G. Scoles, J. Appl. Mech. (submitted).
[15] J. W. Cahn and J. E. Hilliard, J. Chem. Phys. **28**, 258 (1958).
[16] S. D. Evans and A. Ulman, Chem. Phys. Lett. **170**, 462 (1990).
[17] S. D. Evans, E. Urankar, A. Ulman, and N. Ferris, J. Am. Chem. Soc. **113**, 4121 (1991).
[18] D. H. Parker, M. E. Bartram, and B. E. Koel, Surf. Sci. **217**, 489 (1989).
[19] W. Lu and Z. Suo, J. Mech. Phys. Solids **49**, 1937 (2001).
[20] G. Binnig, M. Despont, U. Drechsler, W. Häberle, M. Lutwyche, P. Vettiger, H. J. Mamin, B. W. Chui, and T. W. Kenny, Appl. Phys. Lett. **74**, 1329 (1999).
[21] M. Despont, J. Brugger, U. Drechsler, U. Dürig, W. Häberle, M. Lutwyche, H. Rothuizen, R. Stutz, R. Widmer, G. Binnig, H. Rohrer, and P. Vettiger, Sens. Actuators A **80**, 100 (2000).
[22] J. A. Stroscio and D. M. Eigler, Science **254**, 1319 (1991).
[23] S. Y. Chou and L. Zhuang, J. Vac. Sci. Technol. B **17**, 3197 (1999).
[24] E. Shäffer, T. Thurn-Albrecht, and T. P. Russell, Nature (London) **403**, 874 (2000).